Earth-Science Reviews 235 (2022) 104264

Contents lists available at ScienceDirect

Earth-Science Reviews

journal homepage: www.elsevier.com/locate/earscirev

Thallium in environmental compartments affected by acid mine drainage (AMD) from the Iberian Pyrite Belt (IPB): From rocks to the ocean

Carlos R. Cánovas *, María Dolores Basallote, Francisco Macías, Manuel Olías, Rafael Pérez-López, José Miguel Nieto

Department of Earth Sciences & Research Center on Natural Resources, Health and the Environment, University of Huelva, Campus 'El Carmen', 21071 Huelva, Spain

ARTICLE INFO

Keywords:
Weathering
Metal cycle
Sulfide oxidation
Thallium mobility
Metal transport

ABSTRACT

This works investigates the origin, behavior and fate of Tl in acid mine drainage (AMD) affected areas at catchment scale, following the path from rocks to the ocean. To address this issue, comprehensive data set of Tl in rocks, waters, secondary minerals, plants and other environmental compartments is presented, using the Iberian Pyrite Belt (SW Spain) as representative example. The content of Tl in host rocks (mean of 0.51 mg/kg) exhibits moderate positive correlations with elements such as K and Rb, whereas no correlations were observed in sulfides (27 mg/kg) between Tl, Fe and other metal/loids commonly found in these minerals, such as As, Pb, Cd, Cu or Zn. During sulfide oxidation processes, Tl is mobilized from sulfides, as evidenced by the depletion of Tl in gossans (1.8 mg/kg), and host rock minerals, leading to a Tl enrichment in AMD leachates (mean of 242 μg/L), with concentrations of up to 8.3 mg/L, several orders of magnitude higher than those reported in natural waters. The precipitation of secondary minerals, with large surface areas, may be a sink for Tl, especially in jarosite minerals (8.4 mg/kg). Thallium can be also removed during the treatment of AMD in alkaline passive treatment systems due mainly to sorption processes onto Fe and Al secondary minerals (i.e., schwertmannite and basaluminite, respectively).

Mean Tl contents of 13 mg/kg have been observed in wastes dumped in abandoned mines of the IPB, mainly spoil heaps, slags, roasted pyrite, heap leaching wastes and tailings. However, there is no clear relationship between Tl content and the type of mining wastes. These wastes can suffer weathering, leading to an enrichment of Tl in soils. Previous studies reported that <25% of total Tl is easily extractable, being mainly adsorbed to crystalline Fe oxides in acidic soils and Al oxides in neutral-alkaline soils. Despite this, Tl may be translocated by plants. The translocation of Tl in plants of the IPB has not been properly addressed, however previous studies in other areas showed a low phytoavailability of Tl compared to Cd and Zn, although Tl translocation appears to be strongly controlled by plant species or by differences in Tl speciation. The weathering of rocks, mine wastes and soils may lead to the release of notable amounts of both dissolved and particulate Tl to the hydrosphere. In acidic conditions, Tl seems to be mainly transported by the dissolved phase in AMD-affected streams and rivers, with <15% being transported by the particulate matter. This latter Tl transport may be associated to its incorporation into diatoms and Fe minerals such as jarosite after replacement of Tl^{+} by H^{+} in their structure. Subsequent release by desorption processes from jarosite and diatoms in acidic conditions can occur. This process has also been observed in estuaries affected by AMD, thus, Tl transported by jarosite minerals in the particulate matter and diatoms are released back to the estuarine waters across the salinity gradient due to the increasing proportion of unreactive $TlCl^{0}$ and K^{+} ions, which compete for adsorption sites in jarosite with Tl^{+}. Thus, enhanced transport of Tl to the oceans is observed in AMD-affected systems.

1. Introduction

Thallium (Tl), classified as a non-essential element for living organisms, is a ubiquitous metal in the Earth's crust with a mean concentration of around 0.5 mg/kg (Rudnick and Gao, 2003). Thallium has been historically used as additive in poisons and insecticides, however primary current applications include, among others, medical usage in cardiovascular imaging, gamma radiation detection equipment, high-

* Corresponding author.
E-mail address: carlos.ruiz@dgeo.uhu.es (C.R. Cánovas).

https://doi.org/10.1016/j.earscirev.2022.104264
Received 7 July 2022; Received in revised form 15 November 2022; Accepted 21 November 2022
Available online 25 November 2022

temperature superconductors for wireless communications, infrared detection and transmission equipment and light diffraction in acousto-optical measuring devices (USGS, 2022). World production was close to 10,000 kg in 2021 but due to the difficulty to identify deposits, global reserves are unknown (USGS, 2022). This metal is commonly recovered as a byproduct during processing/roasting of Pb–Cu–Zn and pyrite-rich ore concentrates (Dill, 2010). Thallium is a relatively abundant element in the Earth's crust, in the same range of Sb, with values around 0.2 mg/kg (Rudnick and Gao, 2003), however only 84 Tl minerals are described according to the International Mineralogical Association. In turn, Tl is an abundant minor component in several mineral groups. In this sense, due to its geochemical affinity, Tl^+ can replace K^+, Rb^+, and Sr^+ in K-rich micas and alkali feldspars (Tremel et al., 1997; Law and Turner, 2011). Also, in hydrothermal systems, Tl is commonly bound to sulfides such as pyrite, chalcopyrite, sphalerite, galena or marcasite (Lis et al., 2003). The presence of Tl as impurity in the sulfide crystal structure tends to decrease the mineral resistance to oxidation (Migaszewski and Gałuszka, 2021). Therefore, the majority of Tl in the Earth's crust is associated with potassium and sulfide minerals (Karbowska et al., 2014; Tatsi and Turner, 2014). The weathering of rocks rich in these minerals leads to increasing levels of this metal in soils, waters and sediments. For example, several studies on Tl distribution in French, Austrian and Chinese soils reported Tl concentrations ranging from 0.08 to 1.5 mg/kg (Tremel et al., 1997). Although these values can be greatly exceeded, reaching up to 5.19 mg/kg in some Chinese soils (Liu et al., 2019), they are comparable to those provided by Salminen (2005), who reported a median Tl concentration of 0.66 mg/kg in topsoils from across Europe ($n = 840$). Based on measurements of Tl in a wide variety of large rivers, Nielsen et al. (2005) suggested a global average concentration for river water of 6.6 ng/L and a concentration for non-polluted rivers of 4.5 ng/L. Flegal and Patterson (1985) reported average Tl concentrations in seawater ranging from 10 to 15 ng/L.

Thallium is, like Cd, As, Pb, Hg, Cu or Zn, a highly toxic element classified as priority pollutant by the U.S. Environmental Protection Agency (Belzile and Chen, 2017). The toxicity of Tl is caused by its absorption through the skin and mucous membranes, and its subsequent distribution and accumulation in bones, renal medulla and, eventually, in the central nervous system (Gómez-González et al., 2015). This element, commonly excreted in urine, may also pass through the placenta and transferred to the breastmilk. Thus, the mobility of Tl in the environment may constitute a serious concern, especially in those cases where anthropogenic activities may increase Tl levels in environmental compartments and therefore exposure to living organisms.

Power generating plants, mainly those using brown coal or coal from the Jurassic period, with values of up to 1000 mg/kg (Smith and Carson, 1977), constitute the major sources of Tl emission into the atmosphere (Kazantzis, 2000). After volatilization, Tl is condensed in particles and deposited in the Earth surface, increasing the Tl levels in soils and waterbodies. Other sources of particulate Tl into the environment are cement and smelter plants, whose emission levels are dependent on the Tl content of the raw materials used. Sulfide and coal mining may also notably increase dissolved Tl concentrations in the hydrosphere during acid mine drainage (AMD) processes. In fact, there are some studies describing the occurrence of Tl in AMD impacted regions worldwide. For example, Aguilar-Carrillo et al. (2018) studied the geochemical distribution and mobility of Tl in mining and metallurgical wastes deposited in several mines from Mexico. These authors reported that Tl was usually found associated with labile fractions (i.e. ion-exchangeable and reducible fractions) instead of entrapped in the environmentally-passive residual fraction. Campanella et al. (2018) studied the distribution of aqueous Tl(I)/Tl(III) in an abandoned mining area of Valdicastello Carducci (Italy) as a function of light exposure and solution properties and composition. Ma et al. (2022) discussed the redox transformation of thallium in acidic solutions containing iron, concluding that UV light and H_2O_2 could directly reduce Tl(III) to Tl(I), with the extent of reduction dependent on the presence of Fe(III) and the solution pH, and therefore expanding our current understanding of geochemical Tl redox cycling and its implications for evaluating the ability of Fe to induce oxidation state changes in Tl species in the aquatic environment. Casiot et al. (2011) reported Tl concentrations of up to 534 μg/L in a river impacted by AMD downstream from the abandoned Carnoulès Mine (France) and its sorption on Fe hydroxides. These values are around five orders of magnitude higher than those found in natural river waters. Recently, Cánovas et al. (2021) studied the evolution of the dissolved and particulate Tl concentration in the acidic Tinto River (Iberian Pyrite Belt, IPB; SW Iberian Peninsula) and reported an annual dissolved Tl load to the Atlantic Ocean of around 140 kg. However, to the best of our knowledge, there are no comprehensive studies describing the sources and fate of Tl in AMD affected areas at catchment scale, studying its behavior within the different environmental compartments in the path from the rocks to the ocean. In this sense, the IPB can be considered as a natural laboratory to understand the behavior of Tl in the environment, especially its mobility in rocks and soils and its transference to the water bodies.

2. Material and methods

2.1. Site description

The IPB extends from Seville in South Spain to the Atlantic Ocean coast in South Portugal (approximately 200 km long and 40 km wide) and consists of three distinctive lithological units: the Phyllite-Quartzite Group (PQ), the Volcano-Sedimentary Complex (VSC) and the Culm Group (CG). The PQ group is composed of a thick sequence of shales and quartzites of upper Devonian age while VSC materials (upper Devonian–lower Carboniferous age) are composed of a volcanic sequence, with a very variable thickness that can reach nearly 1300 m (Tornos, 2006), with alternating episodes of felsic (dacites and, in lower proportion, rhyolites) and mafic rocks (occurring as basaltic sills or small stocks) intercalated in a sedimentary and volcano-sedimentary sequence of shales. Felsic rocks are dominant (60%), with similar but lower proportions (20% each) of mafic rocks and shales (Tornos, 2006). The VSC only crops out 25% of the total surface of the IPB and changes dramatically in a short distance due to the intrusive character of some igneous rocks, the abundance of thrusts defining the major contacts and the existence of several paleogeographic domains (Tornos, 2006). The CG is a detrital unit of synorogenic turbidites of up to 3000 m thick, mainly composed of shales and conglomerates of Carboniferous age.

The VSC hosts numerous massive and polymetallic sulfide deposits with original reserves estimated at around 2000 Mt. (Almodóvar et al., 2019). Among them, one of the largest individual deposits of polymetallic sulfides is found, the Riotinto mining district, with original reserves exceeding 500 Mt. Other deposits of importance (above 100 Mt) are: Tharsis, La Zarza, Sotiel, Masa Valverde, Aznalcóllar and Las Cruces in Spain, and Aljustrel and Neves-Corvo in Portugal. In addition, there are around 50 deposits of lower importance distributed within the IPB. Pyrite is the most abundant mineral in the massive sulfide deposits, with the presence of other sulfides such as sphalerite, galena, arsenopyrite and chalcopyrite but in much lower proportions. Tornos (2006) differentiated two types of massive sulfide deposits according to the country rocks: 1) shale-hosted orebodies at the southern part of the IPB with low base metal grades, a stratiform morphology and fine grain sulfides; and 2) orebodies associated with felsic volcanoclastic rocks, located in the northern area of the IPB, characterized by a clear zonation, with zones of enrichment in Cu and others in Zn and Pb (Tornos, 2006). At a regional scale, hydrothermal metamorphism modified the original volcanic and subvolcanic rocks of the IPB (Sáez et al., 1999), while at a local scale, strong hydrothermal alteration occurs related to stringer zones extending below the massive sulfide lenses, with an inner chloritic zone and a peripheral sericitic zone around the sulfide deposits (e.g. Leistel et al., 1998; Tornos, 2006). The chloritic zone is characterized by an extreme leaching of Ca, Na and K, and enrichment in Al, Fe and Mg, whereas in

the sericitic zone the loss of Ca and Na is accompanied by enrichment in K and Al (Almodóvar et al., 1998).

Due to its mineral richness, the IPB has been discontinuously exploited since 3000 BCE for the extraction of mainly gold, silver and copper (Nocete et al., 2005). The Roman period constituted an important development of mining exploitation, whose traces remain today throughout the IPB. Afterwards, mining activity decreased, continuing sporadically during the Visigothic and Arab dominations and the Middle Ages. In the middle of the XIX century, mining activity was restored and sulfide deposits were more intensively exploited coinciding with the Industrial Revolution until now. Then, nearly one hundred mines have been active during 19th and 20th centuries with a total output of 300 Mt. of massive and polymetallic ores for the extraction of mainly S, Cu, Pb and Zn (Sáez et al., 1999). The intense mining activity developed in the IPB has left a huge environmental legacy; around 30.4 km^2 of waste dumps, 8.19 km^2 of tailing dams, 7.1 km^2 of open pits, and 2.79 km^2 of mining infrastructures are found only at the Spanish part of the IPB (Grande et al., 2013).

Oxidation of sulfides contained in mine galleries, open pit walls and mine wastes has led to severe pollution by AMD of the water bodies draining the IPB. The most significant examples of AMD pollution are the Tinto and Odiel Rivers, which are acidic and very rich in metals and metalloids (mean values of 3.9 and 145 mg/L of Fe, 51 and 90 mg/L of Zn, 12 and 88 mg/L of Cu, 0.2 and 4.7 mg/L of As, etc. for the Odiel and Tinto Rivers respectively; Nieto et al., 2013). The low pH values (mean values of 3.64 and 2.82; Cánovas et al., 2007) recorded by both rivers along their water course cause a large deliver of metals and metalloids from AMD-producing sites to their common estuary, known as Ria de Huelva. It is estimated that around 7900 t of Fe, 5800 t of Al, 3500 t of Zn, 1700 t of Cu, 1600 t of Mn and minor quantities of other metals are annually transported in the dissolved phase by both rivers (Olías et al., 2006). This pollutant load is increased during flood events, when the transport of particulate matter especially rich in Fe, As, and Cr, to the estuary is significant (Cánovas et al., 2012).

2.2. Sampling and analytical techniques

A total of 365 aqueous samples were obtained from different locations, including AMD sources, rivers and streams, estuarine and seawaters. AMD, river and stream waters were collected in different points within the Tinto and Odiel river basins (Fig. SM1) during the period (2011−2021), while estuarine and seawater data was obtained during sampling campaigns performed from 2017 to 2019. Sample-containing bottles were washed in 10% (*v*/v) nitric acid (HCl was used instead for collecting seawater) and then rinsed with milli-Q water prior to sampling. Samples were filtered through 0.22 μm, subsequently acidified with suprapure nitric acid (Merck) to pH < 2 and stored in a refrigerator until analysis. Temperature, specific conductivity, pH and redox potential (ORP) of waters were determined in situ. Redox potential values were corrected to obtain the potential referred to the H electrode (Nordstrom and Wilde, 1998). The equipment was checked and calibrated prior to carrying out the measurements. A total of 195 solid samples (i.e., mining wastes, Fe precipitates, sediments and evaporitic sulfate salts) were collected during the same time period as freshwater samples, and dried at room temperature, before performing a chemical and mineralogical characterization. For the chemical analysis, samples were digested using multiacid digestion until total dissolution and subsequent analysis of the digestate. The solids were mineralogically characterized by X-ray diffraction (XRD) using a Bruker D8 Advance X-ray diffractometer with Cu Kα radiation (20 mA, 40 kV and a step size of 2° 2θ/min, 3–65°), and by an environmental scanning electron microscope coupled with a dispersive energy detector (ESEM-EDS; FEI, QEMSCAN 650F).

Major elements (Al, Ca, Cu, Fe, K, Mg, Mn, Na, S, Si, and Zn) were analyzed using inductively coupled plasma optical emission spectroscopy (ICP-AES) on a Jobin Yvon (JY ULTIMA 2) spectrometer. Trace elements (As, Ba, Be, Cd, Co, Cr, Li, Ni, P, Pb, Rb, Sb, Sr, Sn, Ti, Tl, U, and V) were analyzed by iCAP TQ inductively coupled plasma mass spectroscopy (ICP-MS), although in this work only the most relevant elements are included. In order to evaluate the analytical precision, a triplicate analysis was performed, being differences below 5% in all cases. The analytical accuracy was also assessed by the analysis of reference materials (i.e., NIST-1640, SLEW-3, CASS-6, NASS-7). A comparison between certified and measured values can be seen in Table SM1. All elements in blanks were below the detection limit of the technique which were analyzed during each analytical sequence. The chemical composition of liquid (i.e., AMD, estuarine and coastal waters) and solid samples (i.e., sulfides, gossans, evaporitic sulfate salts, AMD precipitates and mine wastes) can be seen in the Supporting Information.

2.3. Data acquisition and treatment

In addition to geological samples (i.e., waters, sediments, precipitates, rocks, wastes) collected by the research group, Tl information has been collected through different sources. For example, chemical data from 345 samples of local host rocks was obtained from ITGE (1999) and Codeço et al. (2018). Chemical information from gossan samples was extended from data ($n = 12$) reported by Hunt et al. (2016). An exhaustive search of works dealing with Tl distribution in AMD sites and other environments was conducted using the indexed databases Web of Science (WoS; http://www.webofknowledge.com/) and SCOPUS (http://www.scopus.com/). In addition, a comprehensive search was also performed in international government agencies (e.g. European Union, USEPA, and USGS). The procedure of literature retrieving was initiated in both databases introducing initially the terms thallium and distribution (2781 documents), refining the search with other terms such as river (216 documents), rocks (172), ocean (79 documents), estuaries (89 documents), sulfide mining (53 documents) and AMD (10 documents). Statistical analysis was performed using XLSTAT Basic (Addinsoft). Spearman's correlation coefficient was used since the concentrations do not exhibit a normal distribution (Davis, 2002).

3. Results and discussion

3.1. Thallium content in rocks and oxidation products

Owing to its chalcophilic and lithophilic properties, the occurrence of Tl in the IPB may be mainly associated with the high concentration of sulfides, and other host rock minerals such as K-rich micas and alkali feldspars. The mean content of Tl in the host rock, mainly acidic volcanic rocks, is of 0.51 mg/kg (median value of 0.28 mg/kg; Table 1). In general, Tl is enriched within K^+-bearing silicates (Rader et al., 2018). Because bonding is predominantly ionic, the atoms of alkaline earth elements behave approximately as hard spheres containing a fixed-point charge at their centers, thus the factors that most govern their behavior in igneous rocks are ionic radius and charge (White, 2013). In this sense, K, Rb, Cs, Sr, and Ba, are often collectively termed the large-ion-lithophile (LIL) elements, and commonly have a similar behavior in igneous rocks. Therefore, a common trend between Tl and these elements should be expected in volcanic rocks of the IPB. Fig. 1 represents the concentration of Tl with respect to other elements in the host rocks, while Table SM2 displays the Spearman correlation coefficients. As shown in Fig. 1, it can be clearly seen a correlation between Tl, Rb ($R^2 = 0.63$), K ($R^2 = 0.53$), Ba and Si ($R^2 = 0.55$), U ($R^2 = 0.51$) and Th ($R^2 = 0.54$). On the other hand, an inverse relationship seems to be observed between Tl, and Sr, Na_2O and Fe_2O_3 (Table SM2). Concerning the typology of volcanic rocks (i.e. acid, intermediate and basic), no differences were observed in Tl distribution with respect the silica content (Fig. 1).

The mean content of Tl in sulfides collected in the main mines of the IPB (Fig. SM1) is noticeably higher than that observed in volcanic rocks

Table 1
Basic statistics of Tl concentrations in main environmental compartments studied within the IPB.

	Host rock	Sulfide	Gossan	AMD precipitates	Wastes	Sulfate salts	AMD	Estuarine waters	Coastal waters
	mg/kg	*mg/kg*	*mg/kg*	*mg/kg*	*mg/kg*	*mg/kg*	*μg/L*	*μg/L*	*ng/L*
n	343	37	59	25	55	19	252	77	36
Minimum	0.05	0.10	0.10	0.10	0.02	0.50	0.10	0.02	10
Maximum	9.2	129	18	46	59	49	8313	5.0	18
Mean	0.51	27	1.8	8.4	12.5	6.0	242	0.51	14
Median	0.28	12	0.40	1.5	7.02	3.6	6.4	0.17	14
Standard Deviation	1.1	35	3.1	16	14	11	1080	1.0	2.3
Percentile 25	0.14	3.0	0.20	0.20	3.05	1.5	1.9	0.09	12
Percentile 75	0.49	34	2.1	5.1	15.8	4.5	35	0.43	16

of the IPB, with 27 mg/kg (interquartile range of 3.0 to 34 mg/kg, Table 1). These values agree well with other sulfide deposits reported worldwide (e.g., 19–56 mg/kg, Yang et al., 2009). The occurrence of Tl in sulfides has been previously associated to Pb^{2+} and As^{3+} bearing sulfides, while Fe bearing sulfides generally have little to no Tl enrichment (Rader et al., 2018). Fig. 2 shows the relationship between Tl and some elements commonly found in sulfides of the IPB as major or minor components. As can be clearly seen, there is no apparent correlation between Tl and Fe sulfides ($R^2 = 0.16$; Table SM3), as reported by Rader et al. (2018). However, no correlations were neither observed between Tl, As, ($R^2 = 0.20$), and Pb ($R^2 = 0.06$), nor other metals present in sulfides except slightly for Zn ($R^2 = 0.56$), Sb ($R^2 = 0.50$), and Cu ($R^2 = 0.49$) (Table SM2).

Sulfides are stable in reducing conditions, however when they are naturally exposed to atmospheric conditions, sulfide oxidation takes place (Eq. 1–2), leading to the formation of acid rock drainage (ARD) and oxidized rocks commonly known as gossans (Eq. 3) which are rich in Fe oxyhydroxides and oxides (i.e. goethite and hematite, respectively). These reactions are highly enhanced during mining activities, which promote the exposure of sulfide to oxygen, giving rise to acid mine drainage (AMD) processes. The acidity released during these reactions causes the dissolution of host rock minerals, which may also host trace concentrations of Tl. Therefore, during these reactions Tl is commonly partitioned among these oxidation products.

$$FeS_2(s) + 7/2\ O_2(g) + H_2O \rightarrow Fe^{2+}(aq) + 2SO_4{}^{2-}(aq) + 2H^+(aq) + energy \quad \text{(Eq. 1)}$$

$$Fe^{2+}(aq) + ¼\ O_2(g) + H^+(aq) \rightarrow Fe^{3+}(aq) + ½\ H_2O + energy \quad \text{(Eq. 2)}$$

$$Fe^{3+}(aq) + 2H_2O \leftrightarrow FeOOH(s) + 3H^+(aq) \quad \text{(Eq. 3)}$$

The mean content of Tl in gossans, the main sulfide oxidation product, in samples collected along the main mines of the IPB (Fig. SM1) is of 1.8 mg/kg, with an interquartile range of 0.20 and 2.1 mg/kg (Table 1). It is therefore evident the Tl depletion in gossan with respect to sulfide (27 mg/kg of average, interquartile range of 3.0–34 mg/kg; Table 1). This Tl depletion in gossan, like other elements contained in original sulfides (e.g., S, Mo, Hg, Cd or Se) was previously reported by Capitán (2006). However, maximum values of 18 mg/kg were observed (Table 1), probably associated to incomplete sulfide oxidation. Fig. 3 shows the relationship between Tl in gossans and some selected elements while Table SM4 shows the Spearman correlation coefficients. Unlike other elements such as As or Pb, commonly concentrated in gossan during sulfide oxidation processes, Tl appears not to be especially hosted by gossans (Fig. 3) after sulfide oxidation, as evidenced by the lack of correlation between Tl and Fe ($R^2 = -0.16$). Such correlations were neither observed between Tl and the rest of chalcophile elements (i.e. S, Cu, As and Sb; $R^2 = -0.41$-0.28, Table SM4). Only in the cases of Al ($R^2 = 0.50$) and Rb ($R^2 = 0.43$), an apparent correlation is observed (Table SM4), due probably to the uncomplete dissolution of the host rock during sulfide oxidation. In this sense, high concentrations of Tl in gossans could be attributed to the presence of remnant pyrite by inefficient oxidation or by incongruent dissolution of aluminosilicate contained in the host rocks, which could have retained Tl.

The low contents of Tl observed in gossans suggest a predominant release of this element into the acid waters. The mean Tl content in AMD sources sampled in the IPB (Fig. SM1) is of 242 μg/L, although this value is strongly affected by the extreme Tl concentrations observed in some AMD sources; for instance, a maximum value of 8313 μg/L was observed in the Tharsis mining district, which is similar to that reported in Valdicastello Carducci (Italy, 9000 μg/L; Campanella et al., 2016) and higher than others in the IPB (2318 μg/L; Sarmiento et al., 2018), Greens Creek (Canada, 5900 μg/L; Lindsay et al., 2015), Carnoulès mine (France, 534 μg/L; Casiot et al., 2011), Iron Mountain (US, 200–400 μg/L; Nordstrom et al., 2000) and Pearl River basin (China, 194 μg/L; Liu et al., 2017). Considering the median value, the Tl concentration in AMD sources studied is of 6.4 μg/L (interquartile range of 1.9–35 μg/L; Table 1). These values contrast with those of 4.5 ng/L reported by Nielsen et al. (2005) for non-contaminated streams, 3 orders of magnitude lower than those observed in AMD samples.

Fig. 4 and Table SM5 shows the relationships between Tl and some elements in AMD samples and their correlation coefficients. The mobility of Tl in AMD systems seems to be strongly controlled by acidity. This fact can be clearly seen in Fig. 4, where an inverse relationship between Tl and pH ($R^2 = -0.61$) is observed. Consequently, the maximum values of Tl (8313 μg/L) were observed at pH values close to 0. The importance of sulfides as Tl contributor to mine waters appears to be clear; high correlation coefficients are observed between Tl and Fe ($R^2 = 0.81$), As ($R^2 = 0.78$), S ($R^2 = 0.78$) and to a lesser extent Cu ($R^2 = 0.65$), Cd ($R^2 = 0.63$), Zn ($R^2 = 0.61$) and Pb ($R^2 = 0.58$). In the case of lithophile elements, no correlations were observed with K, Rb and Al (Fig. 4). The same affinity observed for Tl, Fe, As or Pb in AMD could be linked to the same origin in sulfides. The lack of correlation between Tl and these elements in sulfides (Table SM3) could be related to a nugget effect of Tl in these minerals. Thus, the complete dissolution of Tl-carrier sulfides may cause significant correlation of Tl with these elements in AMD, despite the lack of correlations in bulk sulfides.

During the dissolution of sulfides and gangue minerals significant amounts of dissolved cations and anions are released into waters. If these ions reach saturation levels, the precipitation of secondary minerals can take place. These secondary minerals possess large surface areas; thus, they may adsorb or coprecipitate significant quantities of trace elements including metals and metalloids (Lottermoser, 2010), among them Tl. In this sense, jarosite has been reported as a strong scavenger not only of Tl^+, due to its similarity in size and charge with K^+, but also for Tl^{3+} by Fe^{3+} substitution (Dutrizac et al., 2005). The precipitation of this mineral, widely reported in the IPB (e.g. Sánchez España et al., 2005; Cánovas et al., 2007; López-Arce et al., 2019), is expected to occur under oxidizing, ferric and sulfate-rich, and acidic ($pH < 3$) environments, although its stability is limited by conversion to more stables phases such as goethite or hematite (Barrón et al., 2006; Ryu and Kim, 2022). Saturation indices (SI) of AMD leachates in the IPB indicate oversaturation of waters with respect to jarosite (median value of SI of 5.8, interquartile range (IR) of 3.9–7.0; $n = 225$) over schwertmannite (SI of −1.7, IR of −7.0-1.9). Thus, the mean Tl content in AMD

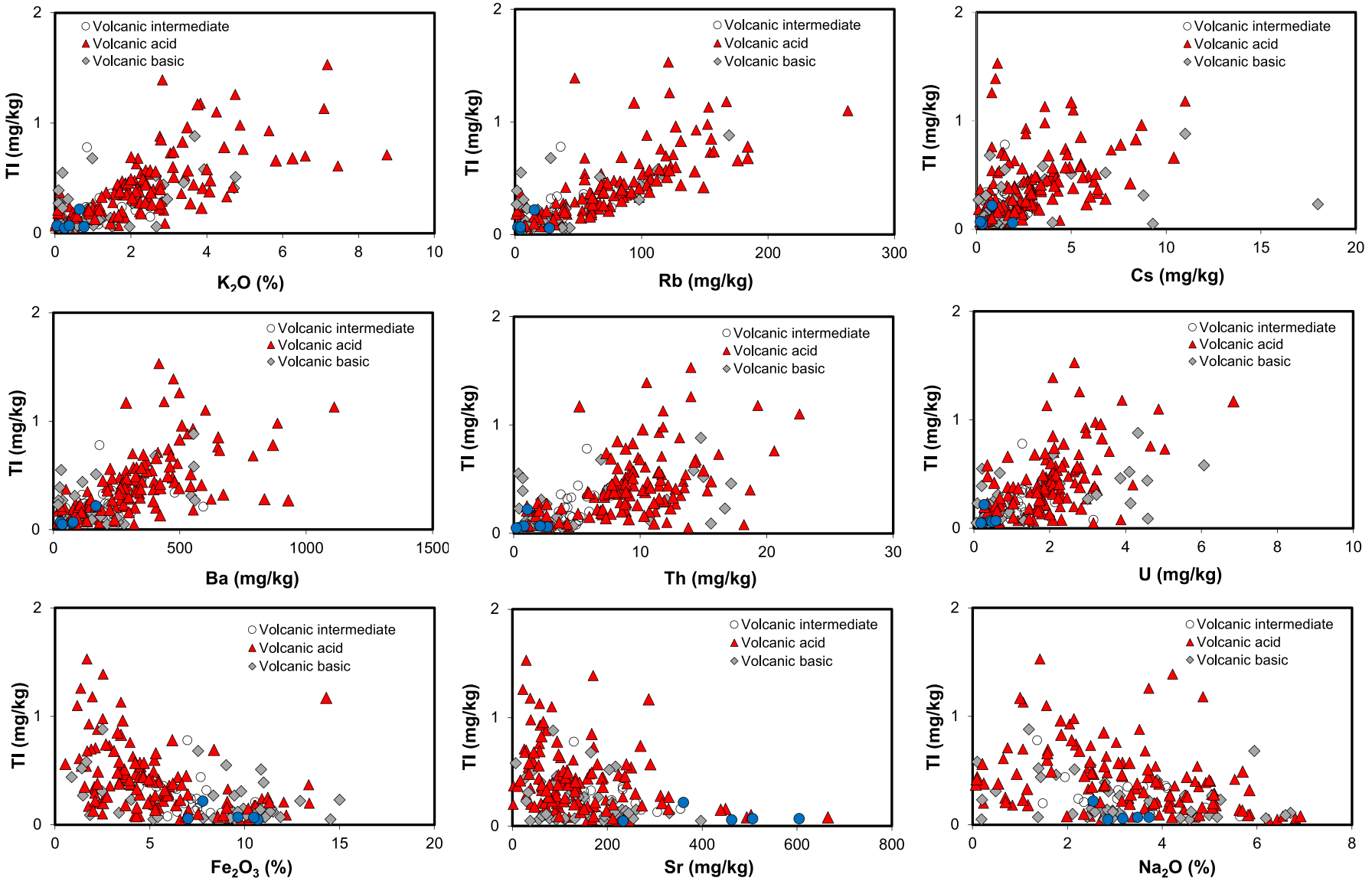

Fig. 1. Relationship between Tl concentrations and other elements in volcanic rocks of the IPB (from ITGE, 1999 and Codeço et al., 2018), classified according to their silica content (i.e., basic (45–52%), intermediate (52–63%) and acid (>63%)).

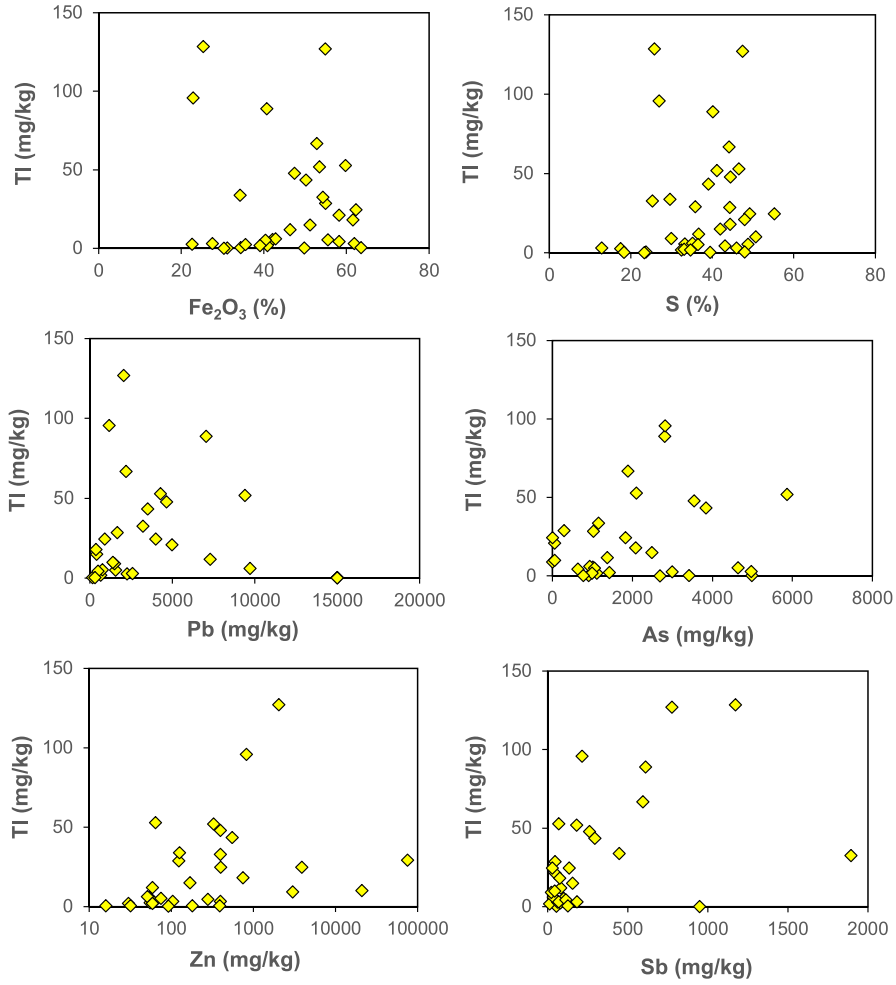

Fig. 2. Relationship between Tl concentrations and some elements in sulfides of the IPB (results from this study).

precipitates studied along the main mines and watercourses of the IPB (Fig. SM1), composed mainly of jarosite and to a lesser extent schwertmannite, is of 8.4 (median values of 1.5 mg/kg, interquartile range of 0.20–5.1 mg/kg; Table 1), with maximum values of 46 mg/kg in jarosite-rich samples. Jarosite may transform with time into more stable mineral phases, such as goethite, remaining most metals in the solid phase during this ageing process (Barrón et al., 2006; Ryu and Kim, 2022). However, the fate of Tl during this mineral transformation remains unknown and should be therefore addressed.

The precipitation of other secondary minerals may be also a sink for Tl in AMD environments. For example, the precipitation of evaporitic sulfate salts constitutes a transient storage of sulfate, acidity and metal/loids. These minerals, formed by evaporation of highly acidic sulfate waters on wet surfaces, seeps and rock fractures, slow down metal pollution in AMD environments, but only temporarily until the arrival of rainfalls, when the dissolution of these salts leads to dramatic episodes of metal pollution (e.g. Alpers et al., 2000; Cánovas et al., 2010). Despite the existence of studies dealing with the formation and chemical composition of sulfate salts in the IPB (e.g. Buckby et al., 2003; Sánchez España et al., 2005; Romero et al., 2006), the presence of Tl in these efflorescent sulfate salts has not been previously reported. Samples collected in different mine sites of the IPB (Fig. SM1) reveal the affinity of these minerals to incorporate Tl if this element is abundant in the initial solution; up to 49 mg/kg of Tl was observed in sulfate salts (interquartile range of 1.5–4.5 mg/kg; Table 1). In the same way, Tl accumulated in evaporitic sulfate salts would be released back to watercourses during the first rainfalls after summer.

3.2. *Thallium distribution in sulfide mine wastes*

Thallium could be also mobilized during mineral extraction and processing in mining areas. In this sense, Chen et al. (2013) reported the mobility of Tl during the roasting of Tl-bearing pyrite to obtain sulfuric acid; 40% of Tl initially contained in pyrite was mobilized during the roasting, while the remaining 60% remained relatively stable in the residual phase. However, the ore mineralogical composition and the temperature of roasting seem to be critical factors in the mobility of Tl during mineral processing. This issue was addressed by Lopez-Arce et al. (2017), who studied the fate of Tl during the roasting of Tl-bearing Fe sulfides from the IPB under controlled conditions in laboratory. These authors reported that sulfide oxidation leads to the formation of Fe oxides rich wastes with different concentrations of Tl. On the one hand, samples with high amounts of quartz (>50%) and lower sulfur content (<30%) mainly developed hematite and concentrated Tl contents from 10 to 72 mg/kg as a function of the firing temperature, rising up to 900 °C. On the other hand, samples with lower contents of quartz (<12%) and higher sulfur content (>35%) led to the formation of magnetite, and accumulated lower amounts of Tl (from 10 to 29 mg/kg at 400–500 °C and from to 1 to 4 mg/kg at 700–900 °C). More recently, López-Arce et al. (2019) suggested that geogenic Tl might be originally hosted by pyrite structure, and after roasting a transference of Tl to Tl(I)-substituted jarosite is observed.

The exposure of mine wastes (e.g., roasted pyrite, spoil heaps, slags, tailings, etc.) to weathering may constitute a significant source of Tl to soils and water courses, especially in areas historically affected by

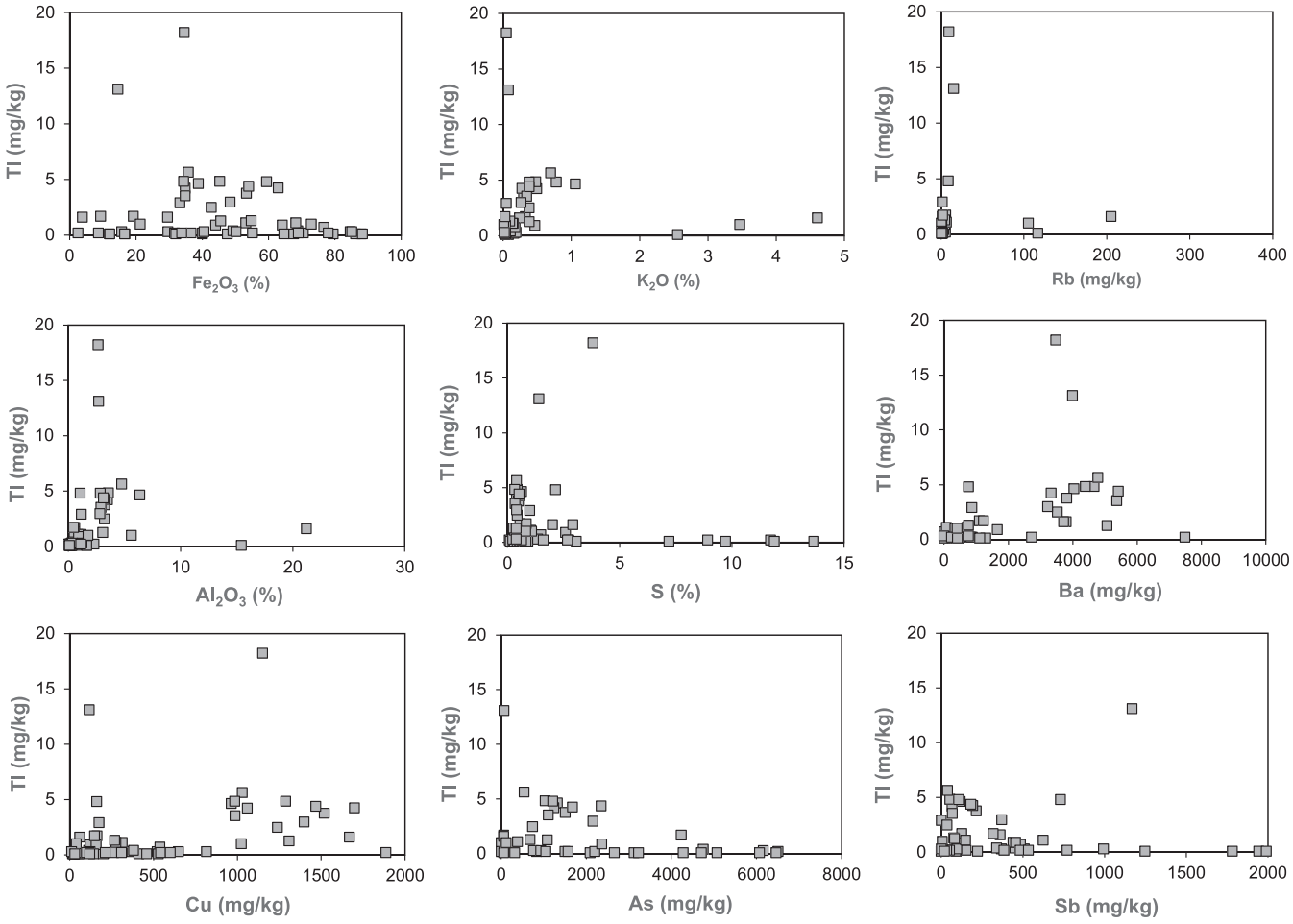

Fig. 3. Relationship between Tl concentrations in gossan and some selected elements (from Hunt et al., 2016 and results of this study).

mining. For example, Yin et al. (2021) revealed that long-term leaching and weathering of tailings can lead to the increased acid-extractable and oxidizable fractions of Tl, and that the exposure and dissolution of Tl-containing sulfides would largely enhance the flux of Tl release. A mean Tl content of 8.4 mg/kg has been observed in wastes deposited along the main mines of the IPB (Fig. SM1) (interquartile range of 3.0–16 mg/kg; Table 1). No correlations were observed between Tl and other elements (i.e. S, Fe, As, Pb, K) neither the Fe mineral type (i.e., pyrite, jarosite, hematite, goethite) in mine wastes. However, the most striking fact is the inverse relationship between the grain size and Tl concentrations when mine wastes are subjected to traditional leaching test with waters (e.g., EC-12457 (CEN, 2002); solid:liquid ratio of 1:10 in agitation for 24 h) to study their reactivity upon rainfalls; the smaller size the higher concentration of Tl in the extraction (Fig. 5). This fact has serious environmental implications due to the greater specific surface of smaller particles, leading to a higher reactivity to weathering agents.

3.3. Soil pollution and Tl translocation in plants

Physical weathering of mine wastes may cause soil pollution. Álvarez-Ayuso et al. (2013) studied the distribution and mobility of Tl in soils impacted by sulfide mine wastes in central Spain and reported that Tl in soils is not of great concern since the mobilizable content represents only a small fraction of the total content. These results agree well with those of López-Arce et al. (2019), who reported that Tl is mainly concentrated (85–99%) in the residual fraction of soils and sediments affected by pollution from roasting heaps of As and Tl bearing pyrite in the Riotinto mining district (IPB). These authors also reported a decrease in Tl pollution with distance from the heaps. Accidental spills may often cause severe Tl soil pollution episodes. The most outstanding example in the IPB is the Aznalcóllar mine spill in 1998, when approximately 4 million m^3 of acidic water and 2 million m^3 of toxic pyritic mud containing high amounts of heavy metals were released to the Agrio River and then passed to the Guadiamar River. In total, around 100 ton of Tl were released and deposited in soils (Grimalt et al., 1999). Although remediation measures were immediately put into practice to reduce metal pollution in these soils, the total Tl content in the surface horizon increased with respect to the background level >4-fold in the uppermost 10 cm of the soils (Martín et al., 2004). These authors also reported that approximately 75% of total Tl was in non-extractable forms, either as a component of the particles in the tailings or adsorbed to crystalline oxides. In acidic soils, the adsorption of Tl was mainly dominated by iron oxides and in neutral-alkaline soils by aluminum oxides. Enhanced Tl levels in soils affected by sulfide mining contrast with the low concentrations observed in natural soils of the study area (Parviainen et al., 2022).

Although the fraction of easily soluble Tl contained in mine soils seems to be low, some previous studies evidence that Tl may be translocated by plants. For example, Wang et al. (2022) reported Tl concentrations of up to 3.74 and 1.16 mg/kg in cabbage (*Brassica oleracea* L.) and radish (*Raphanus sativus* L.), respectively, that exceeded the maximum permissible level (0.5 mg/kg) for food. This transference of Tl from soils to plant tissues (roots and leaves) may pose a risk of biomagnification or even become cause of death in living organisms; Tl concentrations higher than 200 mg/kg of dry weight in the diet turned to be lethal for cattle (Tremel et al., 1997). Unlike in other mine sites

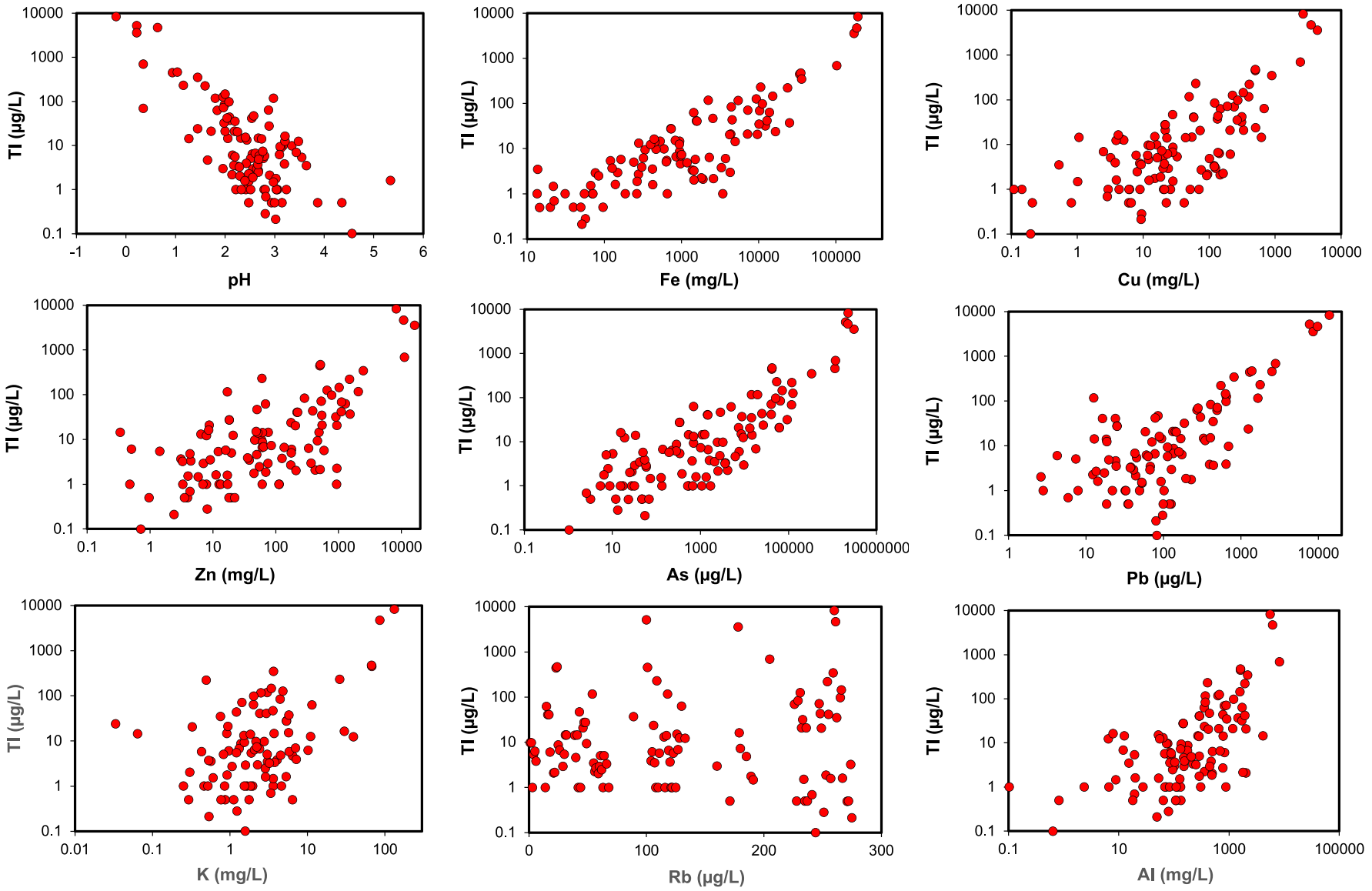

Fig. 4. Relationship between the concentrations of Tl and some elements in AMD waters of the IPB. Data from this study.

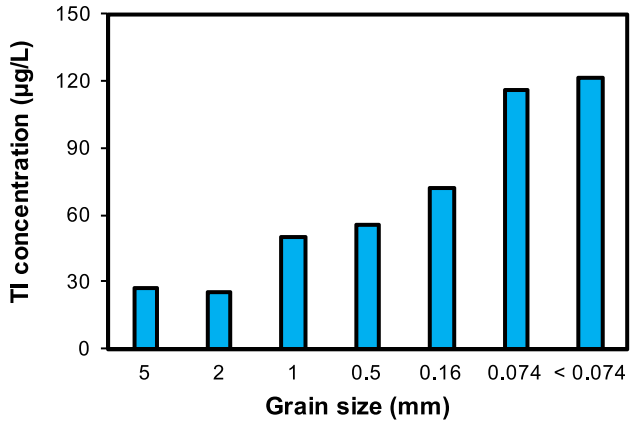

Fig. 5. Relationship between grain size and Tl concentration in leachates obtained from mine wastes according to the standardized EN-12457 procedure (CEN, 2002). Data from this study.

worldwide, translocation of Tl in plants of the IPB has not been properly addressed. Madejón et al. (2007) studied Tl accumulation in plants (i.e., *Brassicaceae* family) growing in polluted soils after the Guadiamar mining spill. These authors report high concentration of Tl in tissues and significant positive correlations between total Tl in soil and Tl in plants, and this accumulation seems to be strongly associated with rainfalls distribution. Álvarez-Ayuso et al. (2013) reported a low phytoavailability of Tl compared to Cd and Zn in soils from central Spain. Different results were obtained by Pavoni et al. (2017) who studied the Tl bioaccumulation in Buckler mustard (Biscutella *laevigata)* nearby a decommissioned Zn—Pb mine in NE Italy. This study evidences a marked capacity of this specie to bioaccumulate trace metals, especially Tl, in the plant tissues. These dissimilar results may be caused by the different plant species or by differences in Tl speciation. At this respect, Krasnodebska-Ostrega et al. (2012) reported a preferential bioaccumulation and translocation of Tl(III) instead of Tl(I) in soils polluted with Tl-rich tailing sediments. Thus, the bioaccumulation of Tl in autochthonous species of the IPB such as *Cistus ladanifer,* Erica *australis L.*, Erica *andevalensis* or Ulex *eriocladus* should be addressed as well as the influence of Tl speciation on translocation rates. In this sense, there are species tolerant to metals such as Erica *australis* L. and Erica *andevalensis*, which have been considered suitable for phytostabilization of metal polluted sites in abandoned mining districts of the IPB (Pérez-López et al., 2014). However, to our knowledge, such factors have not been properly studied until now.

3.4. Thallium mobility during AMD treatment

In spite of being found at lower concentrations than other toxic metal/loids such as Cd, As, or Pb, Tl needs to be removed from mine waters in order to avoid impacts on the environment and human health. Such disposal is commonly accomplished by either active or passive treatments, being the latter usually adopted in abandoned mines (Johnson and Hallberg, 2005). However, there is no consensus about the mobility of Tl during the AMD treatment. For example, Law and Turner (2011) reported a removal of around 65% of Tl during the active treatment of AMD by lime-dosing at the Wheal Jane mine (UK). This value is noticeably lower than that of 95% observed for other pollutants such as Cd, As, Cu, Fe, Mn, Ni, Pb, and Zn upon this treatment and attributed to the higher solubility of Tl(I) than Tl(III), which can be in turn efficiently removed by precipitation.

Torres et al. (2018) studied at lab scale a combined treatment of AMD by successive columns of limestone and barium carbonate dispersed in an inert porous matrix of wood shavings, a technology known as disperse alkaline substrate (DAS) (e.g. Macías et al., 2012; Ayora et al., 2013). While the limestone treatment caused a limited Tl removal (from 38 to 33 µg/L), the barium carbonate treatment was able to remove Tl to values below the detection limit (< 2 µg/L). However, different results have been obtained at full scale by Orden et al. (2021) in the limestone-based passive treatment plant of Mina Esperanza (IPB), near to Concepcion mine (Fig. SM1), proving a high effectiveness removing Tl from mine waters. This treatment plant is initially composed of a natural Fe-oxidizing lagoon (NFOL) of around 100 m^2 (Fig. 6A), which enhances iron oxidation and the removal of Fe (18%) and As (61%) by schwertmannite precipitation. An average removal of 4.9% of Tl was also observed (Fig. 6B) due likely to sorption onto schwertmannite. However, once the water came successively into contact with limestone-filled tanks the removal of Tl was almost complete (Fig. 6B). A detailed examination of the compositional profile of the first limestone tank (TR-1, Fig. 6A), where most dissolved metal/loids are removed (e.g. 99.8% of As, 99.6% of Al, 96.6% of Tl and 76.9% of Fe; Fig. 6C), would allow identifying relationships among elements and inferring the mechanism responsible for Tl depletion inside the tanks. As can be seen in Fig. 6D, there is a surface layer rich in Fe and As due to the intense precipitation of schwertmannite, decreasing their concentration downwards. However, Al and Tl follow a saw tooth pattern with high values found at different levels of the tank (Fig. 6D). The mechanism behind such Tl removal is not clear. Although Tl is commonly incorporated in the structure of jarosite, its presence in schwertmannite, the main Fe mineral formed in DAS treatment, has not been reported. To our knowledge, the incorporation of Tl into Al minerals has neither been reported, and despite following a similar pattern in the tank, both elements show a poor correlation ($R^2 = 0.46$). Therefore, the removal of this element may be related to sorption processes. Lin and Nriagu (1998) modeled, using a two-layer adsorption model, the surface adsorption of Tl(I) and Tl(III) on ferrihydrite. These authors reported an initial adsorption of Tl(I) at pH 3, being completely adsorbed by pH 6. On the other hand, the adsorption of Tl(III) significantly started at pH 4.6 and was completely adsorbed by pH 6.5. Values of pH along the tank remain above pH 6 during the whole operation of the plant, thus these conditions would favor sorption processes onto Fe minerals. The long residence time recorded in the tank (24 h) may favor the intensity of such processes and would explain the better performance of this AMD treatment in relation to others previously reported (e.g. Law and Turner, 2011; Torres et al., 2018). The existence of preferential flow channels inside the tank may also cause the existence of Tl-enriched zones in depth.

3.5. Thallium transport in acidic water courses

The weathering of rocks, mine wastes and soils may lead to the release of notable discharges of both dissolved and particulate Tl to the hydrosphere. Then, different geochemical processes may control the mobility and fate of Tl in aqueous solutions. For instance, sulfide precipitation may scavenge dissolved Tl in sediments of lakes and rivers under anoxic conditions (e.g., Xiong, 2009; Smeaton et al., 2012). Conversely, upon these conditions Tl could be released to the water column after reductive dissolution of Fe and Mn oxides, which may sequester significant concentrations of Tl(III) (Nriagu, 1998). However, despite the oxic conditions observed in AMD systems, Tl(I) may predominate due to the high redox potential of the Tl(III)/Tl(I) couple (Casiot et al., 2011) and also probably due to the UV-mediated reduction of Tl(III) to Tl(I) in acidic Fe(III)-rich solutions (Ma et al., 2022). Different works have dealt with the mobility and transport of Tl in AMD affected water courses. Casiot et al. (2011) studied the mobility of Tl released from the Carnoules mine (France) to the acidic Reigous Creek (pH 3.0–4.5), which feeds the Amous River (pH > 7). These authors reported a low percentage of Tl in the particulate phase (<10%) and a quasi-conservative behavior of Tl due to the low affinity of Tl(I) for Fe oxide phases (i.e. ferrihydrite). More recently, Cánovas et al. (2021)

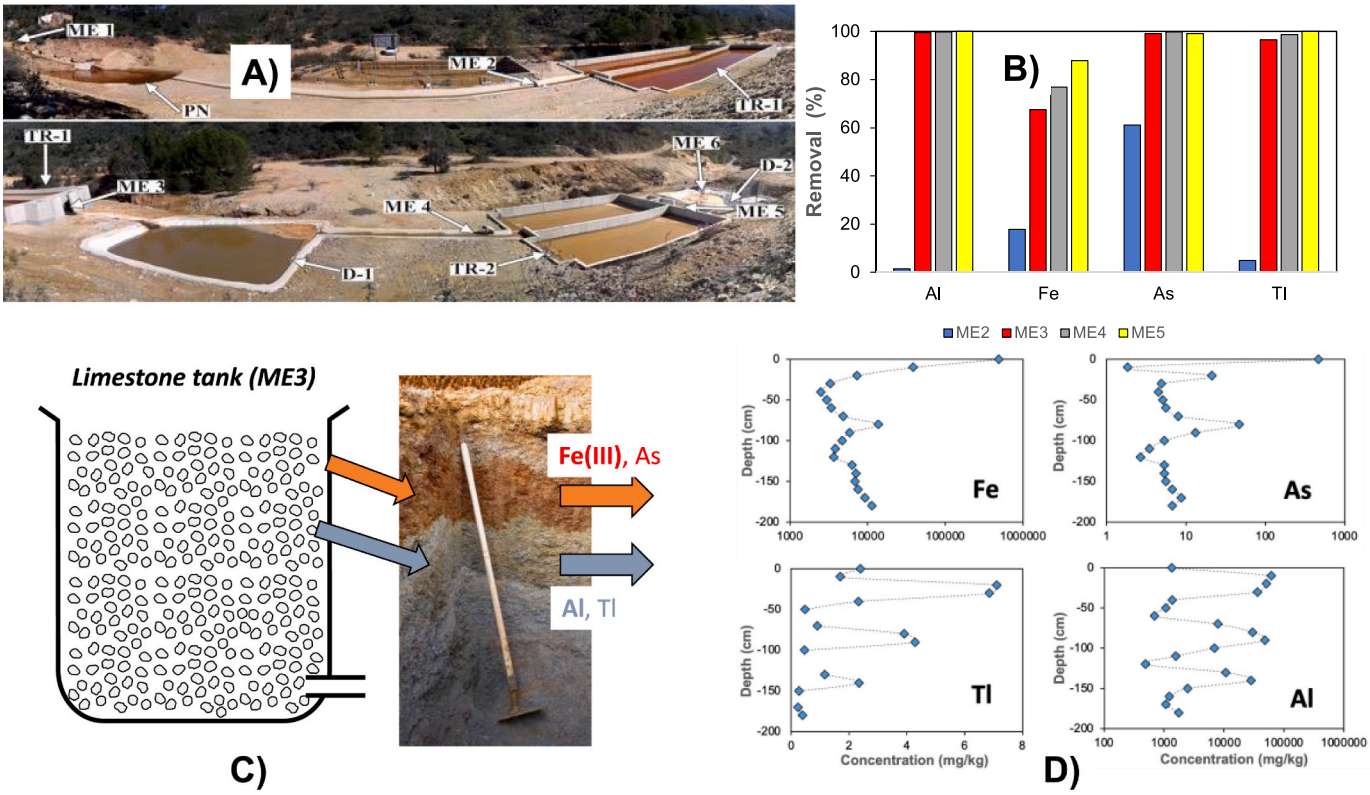

Fig. 6. A) Sketch of the different components of the passive treatment plant of Mina Esperanza, B) removal of Al, Fe, As and Tl during the treatment, C) Sketch of the different mineralogical profiles observed in the limestone tanks (TR1 and TR2) and D) concentrations of Fe, As, Tl and Al in the resulting sludge of the tank profile. Data from this study.

reported the evolution of dissolved and particulate Tl in the acidic Tinto River during a whole hydrologic year, including different flood episodes. These authors reported similar percentages of particulate transport of Tl (average of 12%) as Casiot et al. (2011), with a high correlation with Si and Fe in the particulate matter. In this sense, the precipitation and dissolution of secondary minerals is an important driver of metal concentrations in AMD-affected environments. Lanmuchangite, an aluminosulfate of Tl (i.e., $TlAl(SO_4)_2{\cdot}12H_2O$), has been suggested as potential scavenger of Tl in acid mine waters enriched with aluminum and sulfate (Xiong, 2009). Although AMD waters may be oversaturated with respect to this mineral (Fig. 7A), its occurrence has been only reported in extremely Tl-rich ore deposits (Xiong, 2009) and no described cases of the existence of this mineral in AMD-affected river courses are found in literature. Instead, jarosite (i.e., $KFe_3(SO_4)_2(OH)_6$) seems to play a major role in Tl mobility in AMD systems, since Tl can substitute both K and Fe (III) in the mineral structure (Dutrizac et al., 2005). Fig. 7B shows the evolution of the saturation index (SI) of jarosite in the Tinto River in its middle course (Gadea; Fig. SM1), where oversaturation is observed most of time coinciding with low pH values (<3), except during especially intense flood events (pH > 3), when the precipitation of other Fe mineral phases (e.g. schwertmannite or ferrihydrite) may be favored. Arsenic is a metalloid whose concentration is also strongly controlled by jarosite precipitation in AMD systems (Asta et al., 2010). As can be seen in Fig. 7C, Tl and As followed a similar evolution in the Tinto river waters, exhibiting a high correlation. This fact contrasts with previous findings from Casiot et al. (2011) and Liu et al. (2017) who reported a negative correlation with As, attributed to the higher retention of As in Fe minerals compared with Tl. This discrepancy may be related to the nature of the predominant in-stream precipitating Fe mineral, jarosite in the case of Cánovas et al. (2021) and ferrihydrite, with a lower Tl removal capacity, in Casiot et al. (2011).

In addition, other geochemical processes may affect the mobility of Tl in acidic systems. For instance, the release of acid waters during the washout of soluble salts, especially in semiarid catchments, may induce Tl enrichment in acidic waters. This fact can be seen in Fig. 7C, where a group of samples deviated from the correlation line between As and Tl. Cánovas et al. (2021) attributed this fact to desorption processes from jarosite accumulated in the riverbed by replacement of Tl^+ by H^+ in the mineral structure of jarosite, after the washout of evaporitic salts. However, these authors also hypothesized that this quick Tl release could be related to desorption processes from diatom frustules, ubiquitously found in acidic rivers, which has been reported to scavenge Tl in mine sites (Gómez-González et al., 2015).

3.6. Thallium behavior in AMD-impacted estuaries and coastal waters

After subaerial volcanism (42–700 Mg/a), rivers can be considered the second main source of dissolved and particulate Tl to the oceans, with values ranging from 76 to 380 Mg/a (Nielsen et al., 2017). This transport is especially significant in those rivers impacted by mining activities (e.g., Casiot et al., 2011; Cánovas et al., 2021). In estuaries, sharp geochemical processes take place when freshwaters mix with seawater, leading to intense interaction between suspended particles and the water column (Turner and Millward, 2002). Several studies describing Tl partitioning in estuaries have been published in the last years (e.g., Nielsen et al., 2005; Turner et al., 2010; Anagboso et al., 2013; Böning et al., 2017). These works linked the mobility of Tl to the remobilization of Fe and Mn-rich suspended particles in highly turbid zones occurring at low and intermediate salinities (Nielsen et al., 2005), or the formation of organic complexes (Böning et al., 2017). However, these estuaries do not suffer an intense pressure of mining such as AMD-impacted estuaries. Recently, Cánovas et al. (2022) studied the seasonal distribution and behavior of Tl in the Tinto and Odiel river estuaries, one the most metal polluted in the world due to historical sulfide mining activities. Dissolved Tl concentrations (i.e., from 0.02 to 5.0 μg/L of Tl; Table 1) recorded in this study were up to 3 orders of magnitude higher

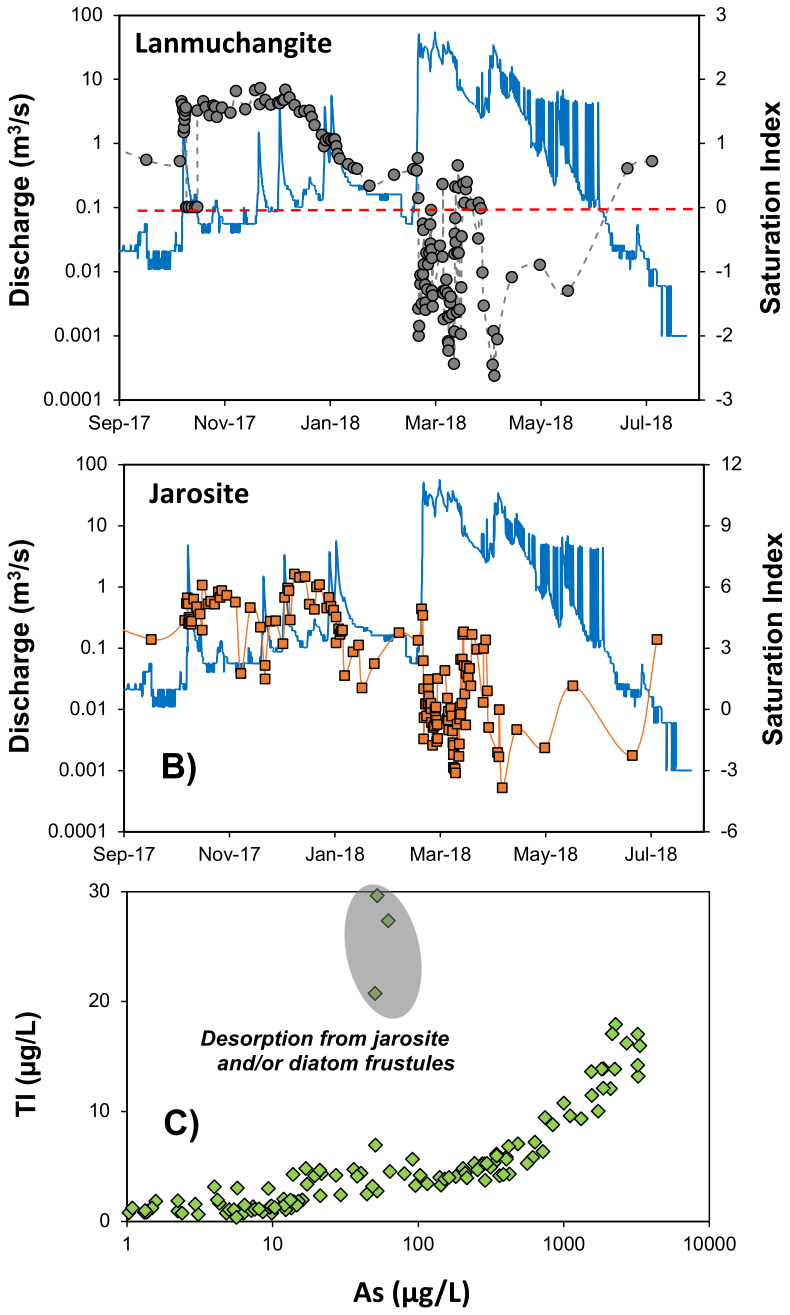

Fig. 7. Saturation indices (SI) of Tinto River waters with respect to lanmuchangite ($Tl^{+}Al(SO_4)_2{\cdot}12H_2O$) (A) and jarosite ($KFe_3^{3+}(SO_4)_2(OH)_6$) (B); and relationship between dissolved Tl and As concentrations in the Tinto River waters (data from Cánovas et al., 2021).

than those observed in other estuaries worldwide and exceeded in some cases the threshold values (i.e., 0.24–0.47 µg/L) established by the USEPA for human health. Unlike other estuaries worldwide, where a fast decrease in dissolved Tl concentration is usually observed due to intense sorption process, increases in Tl concentrations with salinity were observed in the upper reaches of the Tinto and Odiel rivers estuaries, attributed to desorption processes from particulate matter. Both chemical and mineralogical evidences pointed out at jarosite as the main driver of Tl transport in the estuary, releasing Tl back to the water column from across the salinity gradient due to the increasing proportion of unreactive $TlCl^0$ and K^+ ions, which compete for adsorption sites in jarosite with Tl^+ at increasing salinities. This desorption process caused a 6-fold increase in estuarine dissolved Tl concentrations with respect to expected Tl concentrations during the conservative mixing of river and seawaters. These desorption processes can be enhanced if accidental mine spills take place in the catchments, like that occurred in 2017 in the Odiel River (Olías et al., 2019), which increased the dissolved and particulate loads to the estuary and caused a 11-fold increase of estuarine dissolved Tl concentrations. Therefore, Tl behavior in estuaries depends on several factors such as the riverine dissolved Tl concentration, the abundance and properties of organic matter or the amount and nature of particulate matter within the estuary. The release of Tl through estuary may enhance the Tl concentration in coastal waters. In this sense, concentrations in coastal waters within the Gulf of Cádiz ranged from 10 to 18 ng/L (Table 1), close to the highest Tl concentrations in seawater worldwide (Belzile and Chen, 2017).

4. Conclusions

This work reviews the occurrence of Tl in different environmental compartments (e.g., rocks, soils, mine wastes, plants, water courses, estuaries and coastal waters) of AMD-affected systems, focusing on the IPB as representative example worldwide. The mean content of Tl in the host rocks of the IPB, mainly acidic volcanic rocks, is of 0.51 mg/kg (interquartile range -IR- of 0.14–0.49), exhibiting moderate positive correlations with lithophile elements such as K and Rb. The mean content of Tl in sulfides of the IPB is noticeably higher than that observed in volcanic rocks, with 27 mg/kg (IR of 3.0–34 mg/kg), in agreement with other values reported worldwide.

During sulfide oxidation processes, significant amounts of acidity are released which may attack host rocks causing an incongruent dissolution of minerals. The dissolution of both sulfide and host rock minerals leads to the release of Tl to the water courses and the depletion of Tl in gossans, enriching AMD waters in Tl (average of 242 μg/L, IR of 1.9–35 μg/L). The intense oxidation of sulfides in these environments leads to the occurrence of high Tl concentrations (up to 8.3 mg/L), several orders of magnitude higher than those reported in natural waters (commonly below ng/L). This release is strongly controlled by acidity, as evidences the negative correlation between Tl and pH. Unlike in parent materials (i.e., sulfide and host rock minerals), high positive correlations are observed in AMD leachates between Tl and other elements commonly contained in sulfides such as Fe, S, As, Cu or Zn, which pointed to sulfides as predominant source of Tl over host rock minerals.

The precipitation of secondary minerals, with large surface areas, may be a sink of Tl in AMD-affected areas, especially in jarosite minerals. However, redissolution and desorption processes can release back Tl into the watercourses. The treatment of AMD in alkaline passive treatment systems can be also a sink for Tl, as evidenced by previous works, however, the mechanism of removal remains unclear, pointing to sorption processes onto Fe and Al secondary minerals (i.e., schwertmannite and basaluminite) as potential drivers of such depletion from AMD. Mine wastes may also contain significant concentrations of Tl. An average Tl content of 8.4 mg/kg (interquartile range of 3.0–16 mg/kg) has been observed in wastes dumped in abandoned mines of the IPB, mainly spoil heaps, slags, roasted pyrite, heap leaching wastes and tailings. However, there is no clear relationship between Tl content and the type of wastes studied. These wastes can suffer weathering, leading to an enrichment of Tl in soils and subsequent translocation by plants.

The weathering of rocks, mine wastes and soils may lead to the release of notable loads of both dissolved and particulate Tl to the hydrosphere. In acidic conditions, Tl seems to be mainly transported by the dissolved phase in AMD-affected streams and rivers. However, Tl can be significantly incorporated into Fe minerals such as jarosite and even in the structure of diatoms, in some cases temporarily, being released back due to desorption processes by competition for sorption sites. This process has also been observed in estuaries affected by AMD across the salinity gradient due to the increasing proportion of unreactive $TlCl^0$ and K^+ ions, which compete for adsorption sites in jarosite with Tl^+ at increasing salinities. Thus, enhanced transport of Tl to the oceans is observed in AMD-affected systems. However, some questions on Tl mobility in AMD systems need to be answered such as the fate of Tl during Fe mineral transformation processes, the translocation of Tl by plants from contaminated substrates and the influence of Tl speciation on translocation rates or the mechanisms behind Tl removal in treatment systems.

Declaration of Competing Interest

The authors declare that they have no known competing financial interests or personal relationships that could have appeared to influence the work reported in this paper.

Data availability

Raw data is included as Supporting Information

Acknowledgements

This work was supported by the Spanish Ministry of Economy and Competitiveness under the research project TRAMPA (MINECO; PID2020-119196RB-C21) and the Andalusian Regional Government under the AIHODIEL project (*PYC20 RE 032 UHU) within the FEDER program*. C.R Cánovas thanks the Spanish Ministry of Science and Innovation for the Postdoctoral Fellowship granted under application reference RYC2019-027949-I. M.D. Basallote thanks the Spanish Ministry of Science and Innovation for the Postdoctoral Fellowship granted under application reference IJC2018-035056-I. The authors would also like to thank to the Editor Dr. Joan-Albert Sanchez-Cabeza and three anonymous reviewers for the support and comments that notably improved the quality of the original paper. Funding for open access charge: Universidad de Huelva /CBUA

Appendix A. Supplementary data

Supplementary data to this article can be found online at https://doi.org/10.1016/j.earscirev.2022.104264.

References

Aguilar-Carrillo, J., Herrera, L., Gutierrez, E.J., Reyes-Dominguez, I.A., 2018. Solid-phase distribution and mobility of thallium in mining-metallurgical residues: environmental hazard implications. Environ. Pollut. 243, 1833–1845. https://doi.org/10.1016/j.envpol.2018.10.014.

Almodóvar, G.R., Sáez, R., Pons, J.M., Maestre, A., Toscano, M., Pascual, E., 1998. Geology and genesis of the Aznalcóllar massive sulphide deposits, Iberian Pyrite Belt (Spain). Mineral. Deposita 33, 116–136.

Almodóvar, G.R., Yesares, L., Sáez, R., Toscano, M., González, F., Pons, J.M., 2019. Massive sulfide ores in the Iberian Pyrite Belt. Minerals 9, 653.

Alpers, C.N., Jambor, J.L., Nordstrom, D.K. (Eds.), 2000. Sulfate Minerals – Crystallography, Geochemistry, and Environmental Significance. Reviews in Mineralogy and Geochemistry Vol. 40.

Álvarez-Ayuso, E., Otones, V., Murciego, A., García-Sánchez, A., Santa Regina, I., 2013. Zinc, cadmium and thallium distribution in soils and plants of an area impacted by sphalerite-bearing mine wastes. Geoderma 207–208, 25–34. https://doi.org/10.1016/j.geoderma.2013.04.033.

Anagboso, M.U., Turner, A., Braungardt, C., 2013. Fractionation of thallium in the Tamar estuary, south West England. J. Geochem. Explor. 125, 1–7. https://doi.org/10.1016/j.gexplo.2012.10.018.

Asta, M.P., Ayora, C., Roman-Ross, G., Cama, J., Acero, P., Gault, A.D., Charnock, J.M., Bardelli, F., 2010. Natural attenuation of arsenic in the Tinto Santa Rosa acid stream (Iberian Pyritic Belt, SW Spain): the role of iron precipitates. Chem. Geol. 271, 1–12. https://doi.org/10.1016/j.chemgeo.2009.12.005.

Ayora, C., Caraballo, M.A., Macias, F., Rötting, T.S., Carrera, J., Nieto, J.M., 2013. Acid mine drainage in the Iberian Pyrite Belt: 2. Lessons learned from recent passive remediation experiences. Environ. Sci. Pollut. Res. 20, 7837–7853. https://doi.org/10.1007/s11356-013-1479-2.

Barrón, V., Torrent, J., Greenwood, J., 2006. Transformation of jarosite to hematite in simulated Martian brines. Earth Planet. Sci. Lett. 251 (3–4), 380–385. https://doi.org/10.1016/j.epsl.2006.09.022.

Belzile, N., Chen, Y.W., 2017. Thallium in the environment: a critical review focused on natural waters, soils, sediments and airborne particles. Appl. Geochem. 84, 218–243. https://doi.org/10.1016/j.apgeochem.2017.06.013.

Böning, P., Ehlert, C., Niggemann, J., Schnetger, B., Pahnke, K., 2017. Thallium dynamics in the Weser estuary (NW Germany). Estuar. Coast. Shelf Sci. 187, 146–151. https://doi.org/10.1016/j.ecss.2016.12.004.

Buckby, T., Black, S., Coleman, M.L., Hodson, M.E., 2003. Fe-sulphate rich evaporative mineral precipitates from the río Tinto, Southwest Spain. Mineral. Mag. 67, 263–278.

Campanella, B., Onor, M., D'Ulivo, A., Giannecchini, R., D'Orazio, M., Petrini, R., Bramanti, E., 2016. Human exposure to thallium through tap water: a study from Valdicastello Carducci and Pietrasanta (Northern Tuscany, Italy). Sci. Total Environ. 548–549 https://doi.org/10.1016/j.scitotenv.2016.01.010.

Campanella, B., D'Ulivo, A., Ghezzi, L., Onor, M., Petrini, R., Bramanti, E., 2018. Influence of environmental and anthropogenic parameters on thallium oxidation state in natural waters. Chemosphere 196, 1–8. https://doi.org/10.1016/j.chemosphere.2017.12.155.

Cánovas, C.R., Olías, M., Nieto, J.M., Sarmiento, A.M., Cerón, J.C., 2007. Hydrogeochemical characteristics of the Odiel and Tinto rivers (SW Spain). Factors controlling metal contents. Sci. Total Environ. 373, 363–382. https://doi.org/10.1016/j.scitotenv.2006.11.022.

Cánovas, C.R., Olías, M., Nieto, J.M., Galván, L., 2010. Wash-out processes ofevaporitic sulfate salts in the Tinto river: hydrogeochemical evolution andenvironmental impact. Appl. Geochem. 25 (2), 288–301. https://doi.org/10.1016/j.apgeochem.2009.11.014.

Cánovas, C.R., Olías, M., Sarmiento, A.M., Nieto, J.M., Galván, L., 2012. Pollutant transport processes in the Odiel River (SW Spain) during rain events. Water Resour. Res. 48, W06508 (0043-1397/12/2011WR011041).

Cánovas, C.R., Basallote, M.D., Macías, F., Olías, M., Pérez-López, R., Ayora, C., Nieto, J. M., 2021. Geochemical behaviour and transport of technology critical metals (TCMs) by the Tinto River (SW Spain) to the Atlantic Ocean. Sci. Total Environ. 764, 143796 https://doi.org/10.1016/j.scitotenv.2020.143796.

Cánovas, C.R., Basallote, M.D., Macías, F., Freydier, R., Parviainen, A., Pérez-López, R., 2022. Thallium distribution in an estuary affected by acid mine drainage (AMD): the Ría de Huelva estuary (SW Spain). Env. Poll. 306, 119448 https://doi.org/10.1016/j.envpol.2022.119448.

Capitán, M.A., 2006. In: Mineralogía y geoquímica de la alteración superficial de sulfuros masivos en la Faja Pirítica Ibérica. PhD dissertation. University of Huelva, p. 230. http://rabida.uhu.es/dspace/handle/10272/7627.

Casiot, C., Egal, M., Bruneel, O., Verma, N., Parmentier, M., Elbaz-Poulichet, F., 2011. Predominance of aqueous Tl(I) species in the river system downstream from the abandoned Carnoules Mine (Southern France). Environ. Sci. Technol. 45, 2056–2064. https://doi.org/10.1021/es102064r.

CEN, 2002. Characterization of Waste, Compliance Test for Leaching of Granular Wastes Materials and Sludges, Part 2: One Stage Batch Test at a Liquid to Solid Ratio of 10 L/kg-1 for Materials with Particle Size below 4 Mm (Without or with Size Reduction). European Committee of Standardization, p. 28. CEN/TC 292,12/02.

Chen, Y.H., Wang, C.L., Liu, J., Wang, J., Qi, J.Y., Wu, Y.J., 2013. Environmental exposure and flux of thallium by industrial activities utilizing thallium-bearing pyrite. Sci. China Ser. D. 56, 1502–1509. https://doi.org/10.1007/s11430-013-4621-6.

Codeço, M.S., Mateus, A., Figueiras, J., Rodrigues, P., Gonçalves, L., 2018. Development of the Ervidel-Roxo and Figueirinha-Albernoa volcanic sequences in the Iberian Pyrite Belt, Portugal: metallogenic and geodynamic implications. Ore Geol. Rev. 98, 80–108. https://doi.org/10.1016/j.oregeorev.2018.05.009.

Davis, J.C., 2002. Statistics and Data Analysis in Geology. John Wiley & Sons, USA.

Dill, H.G., 2010. The "chessboard" classification scheme of mineral deposits: mineralogy and geology from aluminum to zirconium. Earth Sci. Rev. 100, 1–420. https://doi.org/10.1016/j.earscirev.2009.10.011.

Dutrizac, J.E., Chen, T.T., Beauchemin, S., 2005. The behaviour of thallium(III) during jarosite precipitation. Hydrometallurgy 79, 138–153. https://doi.org/10.1016/j.hydromet.2005.06.003.

Flegal, A.R., Patterson, C.C., 1985. Thallium concentrations in seawater. Mar. Chem. 15, 327–331.

Gómez-González, M.A., Garcia-Guinea, J., Laborda, F., Garrido, F., 2015. Thallium occurrence and partitioning in soils and sediments affected by mining activities in Madrid province (Spain). Sci. Total Environ. 536, 268–278. https://doi.org/10.1016/j.scitotenv.2015.07.033.

Grande, J.A., Valente, T., De la Torre, M.L., Santisteban, M., Cerón, J.C., Pérez-Ostalé, E., 2013. Characterization of acid mine drainage sources in the Iberian Pyrite Belt: base methodology for quantifying affected areas and for environmental management. Environ. Earth Sci. 71, 2729. https://doi.org/10.1007/s12665-013-2652-0.

Grimalt, J.O., Ferrer, M., Macpherson, E., 1999. The mine tailing accident in Aznalcollar. Sci. Total Environ. 242, 3–11. https://doi.org/10.1016/S0048-9697(99)00372-1.

Hunt, J., Lottermoser, B.G., Parbhakar-Fox, A., Van Veen, E., Goemann, K., 2016. Precious metals in gossanous waste rocks from the Iberian Pyrite Belt. Miner. Eng. 87, 45–53. https://doi.org/10.1016/j.mineng.2015.12.002.

ITGE, 1999. Investigación geolológica y cartografía básica en la Faja Pirítica y áreas aledañas a escala 1:50000. https://data.europa.eu/data/datasets/-086dea60-3bf1-4dc6-8aca-8d54bd20face-_100223_full1_es?locale=es accessed on June 21st 2022.

Johnson, D.B., Hallberg, K.B., 2005. Acid mine drainage remediation options: a review. Sci. Total Environ. 338 (1), 3–14. https://doi.org/10.1016/j.scitotenv.2004.09.002.

Karbowska, B., Zembrzuski, W., Jakubowska, M., Wojtkowiak, T., Pasieczna, A., Lukaszewski, Z., 2014. Translocation and mobility of thallium from zinc–lead ores. J. Geochem. Explor. 143, 127–135.

Krasnodebska-Ostrega, B., Sadowska, M., Ostrowska, S., 2012. Thallium speciation in plant tissues—Tl(III) found in Sinapis alba L. grown in soil polluted with tailing sediment containing thallium minerals. Talanta 93, 326–329. https://doi.org/10.1016/j.talanta.2012.02.042.

Kazantzis, G., 2000. Thallium in the environment and health effects. Environ. Geochem. Health 22, 275–280.

Law, S., Turner, A., 2011. Thallium in the hydrosphere of south West England. Environ. Poll. 159, 3484–3489. https://doi.org/10.1016/j.envpol.2011.08.029.

Leistel, J.M., Marcoux, E., Thiéblemont, D., Quesada, C., Sánchez, A., Almodóvar, G.R., Pascual, E., Sáez, R., 1998. The volcanic-hosted massive sulphide deposits of the Iberian Pyrite Belt. Mineral. Deposita 33, 2–30.

Lin, T.S., Nriagu, J.O., 1998. Speciation of thallium in natural waters. In: Nriagu, J.O. (Ed.), Thallium in the Environment, Vol. 29, Advances in Environmental Sci. and Technology. Wiley and Sons, NY, pp. 31–44, 1998.

Lindsay, M.B.J., Moncur, M.C., Bain, J.G., Jambor, J.L., Ptacek, C.J., Blowes, D.W., 2015. Geochemical and mineralogical aspects of sulfide mine tailings. Appl. Geochem. 57, 157–177. https://doi.org/10.1016/j.apgeochem.2015.01.009.

Lis, J., Pasieczna, A., Karbowska, B., Zembrzuski, W., Lukaszewski, Z., 2003. Thallium in soils and stream sediments of a Zn-Pb mining and smelting area. Environ. Sci. Technol. 37, 4569–4572. https://doi.org/10.1021/es0346936.

Liu, J., Wang, J., Chen, Y., Lippold, H., Xiao, T., Li, H., Shen, C.-C., Xie, L., Xie, X., Yang, H., 2017. Geochemical transfer and preliminary health risk assessment of thallium in a riverine system in the Pearl River Basin,South China. J. Geochem. Explor. 176, 64–75. https://doi.org/10.1016/j.gexplo.2016.01.011.

Liu, J., Li, N., Zhang, W., Wei, X., Tsang, D.C.W., Sun, Y., Luo, X., Bao, Z.A., Zheng, W., Wang, J., et al., 2019. Thallium contamination in farmlands and common vegetables in a pyrite mining city and potential health risks. Environ. Pollut. 248, 906–915. https://doi.org/10.1016/j.envpol.2019.02.092.

Lottermoser, B.G., 2010. Mine Wastes: Characterization, Treatment, Environmental Impacts. In: second ed. Springer, Berlin Heidelberg, pp. 1–301.

Lopez-Arce, P., Garcia-Guinea, J., Garrido, F., 2017. Chemistry and phase evolution during roasting of toxic thallium-bearing pyrite. Chemosphere 181, 447–460. https://doi.org/10.1016/j.chemosphere.2017.04.109.

López-Arce, P., Garrido, F., García-Guinea, J., Voegelin, A., Göttlicher, J., Nieto, J.M., 2019. Historical roasting of thallium- and arsenic-bearing pyrite: current Tl pollution in the Riotinto mine area. Sci. Total Environ. 648, 1263–1274. https://doi.org/10.1016/j.scitotenv.2018.08.260.

Ma, C., Huang, R., Huangfu, X., Ma, J., He, Q., 2022. Light- and H2O2-mediated redox transformation of thallium in acidic solutions containing iron: kinetics and mechanistic insights. Environ. Sci. Technol. 56 (9), 5530–5541. https://doi.org/10.1021/acs.est.2c00034.

Macías, F., Caraballo, M.A., Nieto, J.M., Rötting, T.S., Ayora, C., 2012. Natural pretreatment and passive remediation of highly polluted acid mine drainage. J. Environ. Manag. 104, 93–100. https://doi.org/10.1016/j.jenvman.2012.03.027.

Madejón, P., Murillo, J.M., Marañón, T., Lepp, N.W., 2007. Factors affecting accumulation of thallium and other trace elements in two wild brassicaceae spontaneously growing on soils contaminated by tailings dam waste. Chemosphere 67, 20–28. https://doi.org/10.1016/j.scitotenv.2022.154346.

Martín, F., García, I., Dorronsoro, C., Simón, M., Aguilar, J., Ortiz, I., Fernández, E., Fernández, J., 2004. Thallium behavior in soils polluted by pyrite tailings (Aznalcóllar, Spain). Soil Sediment Contam. Int. J. 13 (1), 25–36. https://doi.org/10.1080/10588330490269769.

Migaszewski, Z.M., Gałuszka, A., 2021. Abundance and fate of thallium and its stable isotopes in the environment. Rev. Environ. Sci. Biotechnol. 20, 5–30. https://doi.org/10.1007/s11157-020-09564-8.

Nielsen, S.G., Rehkämper, M., Porcelli, D., Andresson, P., Halliday, A.N., Swarzenski, P. W., Latkoczy, C., Günther, D., 2005. Thallium isotope composition of the upper continental crust and rivers —an investigation of the continental sources of dissolved marine thallium. Geochim. Cosmochim. Acta 69, 2007–2019. https://doi.org/10.1016/j.gca.2004.10.025.

Nielsen, S.G., Rehkämper, M., Prytulak, J., 2017. Investigation and application of thallium isotope fractionation. Rev. Mineral. Geochem. 82 (1), 759–798. https://doi.org/10.2138/rmg.2017.82.18.

Nieto, J.M., Sarmiento, A.M., Cánovas, C.R., Olías, M., Ayora, C., 2013. Acid mine drainage in the Iberian Pyrite Belt: 1. Hydrochemical characteristics and pollutant load of the Tinto and Odiel rivers. Environ. Sci. Pollut. Res. 20, 7509–7519. https://doi.org/10.1007/s11356-013-1634-9.

Nocete, F., Alex, E., Nieto, J.M., Sáez, R., Bayona, M.R., 2005. An archaeological approach to regional environmental pollution in the South-Western Iberian Peninsula related to third millenium BC mining and metallurgy. J. Archaeol. Sci. 32, 1566–1576. https://doi.org/10.1016/j.jas.2005.04.012.

Nordstrom, D.K., Wilde, F.D., 1998. Reduction–oxidation potential (electrode method). National Field Manual for the Collection of Water Quality Data, Book 9, Chapter 6.5. U.S. Geological Survey Techniques of Water-Resources Investigations. U.S. Geological Survey, Reston, VA, 20 pp.

Nordstrom, D.K., Alpers, C.N., Ptacek, C.J., Blowes, D.W., 2000. Negative pH and extremely acidic mine waters from Iron Mountain, California. Environ. Sci. Technol. 34 (2), 254–258. https://doi.org/10.1021/es990646v.

Nriagu, J.O. (Ed.), 1998. Thallium in the Environment. John Wiley & Sons, New York.

Olías, M., Cánovas, C., Nieto, J.M., Sarmiento, A.M., 2006. Evaluation of the dissolved contaminant load transported by the Tinto and Odiel rivers (South West Spain). Appl. Geochem. 21, 1733–1749. https://doi.org/10.1016/j.apgeochem.2006.05.009.

Olías, M., Cánovas, C.R., Basallote, M.D., Macías, F., Pérez-López, R., Moreno González, R., Millán-Becerro, R., Nieto, J.M., 2019. Causes and impacts of a mine water spill from an acidic pit lake (Iberian Pyrite Belt). Environ. Pollut. 250, 127–136. https://doi.org/10.1016/j.envpol.2019.04.011.

Orden, S., Macías, F., Cánovas, C.R., Nieto, J.M., Pérez-López, R., Ayora, C., 2021. Eco-sustainable passive treatment for mine waters: full-scale and long-term demonstration. J. Environ. Manag. 111699. https://doi.org/10.1016/j.jenvman.2020.111699.

Parviainen, A., Vázquez-Arias, A., Martín-Peinado, F.J., 2022. Mineralogical association and geochemistry of potentially toxic elements in urban soils under the influence of mining. Catena 217, 106517. https://doi.org/10.1016/j.catena.2022.106517.

Pavoni, E., Petranich, E., Adami, G., Baracchini, E., Crosera, M., Emili, A., Lenaz, D., Higueras, P., Covelli, S., 2017. Bioaccumulation of thallium and other trace metals in Biscutella laevigata nearby a decommissioned zinc-lead mine (Northeastern Italian Alps). J. Environ. Manag. 186, 214–224. https://doi.org/10.1016/j.jenvman.2016.07.022.

Pérez-López, R., Márquez-García, B., Abreu, M.M., Nieto, J.M., Córdoba, F., 2014. Erica andevalensis and Erica australis growing in the same extreme environments: phytostabilization potential of mining areas. Geoderma 230–231, 194–203. https://doi.org/10.1016/j.geoderma.2014.04.004.

Rader, S.T., Mazdab, F.K., Barton, M.D., 2018. Mineralogical thallium geochemistry and isotope variations from igneous, metamorphic, and metasomatic systems. Geochim. Cosmochim. Acta 243, 42–65. https://doi.org/10.1016/j.gca.2018.09.019.

Romero, A.J., González, I., Galán, E., 2006. The role of efflorescent sulfate salts in the storage of trace elements in stream waters polluted by acid mine drainage: the case of Peña del Hierro, southwestern Spain. Can. Mineral. 44, 1341–1346. https://doi.org/10.2113/gscanmin.44.6.1431.

Rudnick, R.L., Gao, S., 2003. The Composition of the Continental Crust. In: Holland, H. D., Turekian, K.K. (Eds.), Treatise on Geochemistry, Vol. 3. The Crust, Elsevier-Pergamon, Oxford, pp. 1–64. https://doi.org/10.1016/b0-08-043751-6/03016-4.

Ryu, J.G., Kim, Y., 2022. Mineral transformation and dissolution of jarosite coprecipitated with hazardous oxyanions and their mobility changes. J. Hazard. Mat. 427, 128283 https://doi.org/10.1016/j.jhazmat.2022.128283.

Sáez, R., Pascual, E., Toscano, M., Almodóvar, G.R., 1999. The Iberian type of volcanosedimentary massive deposits. Mineral. Deposita 34, 549–570. https://doi.org/10.1007/s001260050220.

Salminen, R. (Ed.), 2005. Geochemical Atlas of Europe. Part 1: Background Information, Methodology and Maps; Geological Survey of Finland: Espoo.

Sánchez España, J., Lopez Pamo, E., Santofimia, E., Aduvire, O., Reyes, J., Barettino, D., 2005. Acid mine drainage in the Iberian Pyrite Belt (Odiel river watershed, Huelva, SW Spain): geochemistry, mineralogy and environmental implications. Appl. Geochem. 20, 1320–1356. https://doi.org/10.1016/j.apgeochem.2005.01.011.

Sarmiento, A.M., Grande, J.A., Luís, A.T., Dávila, J.M., Fortes, J.C., Santisteban, M., Curiel, J., de la Torre, M.L., da Silva, E.F., 2018. Negative pH values in an open-air radical environment affected by acid mine drainage. Characterization and proposal of a hydrogeochemical model. Sci. Total Environ. 644, 1244–1253. https://doi.org/10.1016/j.scitotenv.2018.06.381.

Smeaton, C.M., Walshe, G.E., Fryer, B.J., Weisener, C.G., 2012. Reductive dissolution of Tl(I)-Jarosite by Shewanella putrefaciens: providing new insights into Tl biogeochemistry. Environ. Sci. Technol. 46, 11086–11094. https://doi.org/10.1021/es302292d.

Smith, I.C., Carson, B.L., 1977. Trace Metals in the Environment vol 1: Thallium. Ann Arbor Scientific Publications, Ann Arbor, MI, 1977.

Tatsi, K., Turner, A., 2014. Distributions and concentrations of thallium in surface waters of a region impacted by historical metal mining (Cornwall, UK). Sci. Total Environ. 473–474, 139–146. https://doi.org/10.1016/j.scitotenv.2013.12.003.

Tornos, F., 2006. Environment of formation and styles of volcanogenic massive sulfides: the Iberian Pyrite Belt. Ore Geol. Rev. 28, 259–307. https://doi.org/10.1016/j.oregeorev.2004.12.005.

Torres, E., Lozano, A., Macías, F., Gómez-Arias, A., Castillo, J., Ayora, C., 2018. Passive elimination of sulfate and metals from acid mine drainage using combined limestone and barium carbonate systems. J. Clean. Prod. 182, 114–123. https://doi.org/10.1016/j.jclepro.2018.01.224.

Tremel, A., Masson, P., Sterckeman, T., Baize, D., Mench, M., 1997. Thallium in french agrosystems—I. Thallium contents in arable soils. Environ. Pollut. 95, 293–302. https://doi.org/10.1016/S0269-7491(96)00145-5.

Turner, A., Millward, G.E., 2002. Suspended particles: their role in estuarine biogeochemical cycles. Estuar. Coast. Shelf Sci. 55, 857–883. https://doi.org/10.1006/ecss.2002.1033.

Turner, A., Cabon, A., Glegg, G.A., Fisher, A.S., 2010. Sediment-water interactions of thallium under simulated estuarine conditions. Geochim. Cosmochim. Acta 74, 6779–6787. https://doi.org/10.1016/j.gca.2010.09.004.

USGS, 2022. U.S. Geological Survey, 2022, Mineral commodity summaries 2022: U.S. Geological Survey. https://doi.org/10.3133/mcs2022, 202 p.

Wang, J., Liu, S., Wei, X., Beiyuan, J., Wang, L., Liu, J., Sun, H., Zhang, G., Xiao, T., 2022. Uptake, organ distribution and health risk assessment of potentially toxic elements in crops in abandoned indigenous smelting region. Chemosphere 292, 133321. https://doi.org/10.1016/j.chemosphere.2021.133321.

White, W.M., 2013. Geochemistry. Wiley-Blackwell, Hoboken, NJ (USA).

Xiong, Y., 2009. The aqueous geochemistry of thallium: speciation and solubility of thallium in low temperature systems. Environ. Chem. 6, 441–451. https://doi.org/10.1071/EN08086.

Yang, C., Chen, Y., Peng, P.A., Li, C., Chang, X., Wu, Y., 2009. Trace element transformations and partitioning during the roasting of pyrite ores in the sulfuric acid industry. J. Hazard Mater. 167, 835–845. https://doi.org/10.1016/j.jhazmat.2009.01.067.

Yin, M., Zhou, Y., Tsang, D., Beiyuan, J., Song, L., She, J., Wang, J., Zhu, L., Fang, F., Wang, L., Liu, J., Liu, Y., Song, G., Chen, D., Xiao, T., 2021. Emergent thallium exposure from uranium mill tailings. J. Hazard. Mater. 407, 124402 https://doi.org/10.1016/j.jhazmat.2020.124402.